



Acta Scientiae Veterinariae

ISSN: 1678-0345

ActaSciVet@ufrgs.br

Universidade Federal do Rio Grande do Sul
Brasil

Tejero, Felix; Arias-Mota, Lourdes Lorena; Roschman-González, Antonio; Aso, Pedro María; Finol, Héctor José

Trypanosoma evansi: Ultrastructural Cardiac Muscle and Cardiac Microvasculature Changes in
Experimental Murine Infections

Acta Scientiae Veterinariae, vol. 38, núm. 3, 2010, pp. 279-285

Universidade Federal do Rio Grande do Sul
Porto Alegre, Brasil

Available in: <http://www.redalyc.org/articulo.oa?id=289021902008>

- How to cite
- Complete issue
- More information about this article
- Journal's homepage in redalyc.org

redalyc.org

Scientific Information System
Network of Scientific Journals from Latin America, the Caribbean, Spain and Portugal
Non-profit academic project, developed under the open access initiative

Trypanosoma evansi*: Ultrastructural Cardiac Muscle and Cardiac Microvasculature Changes in Experimental Murine Infections

Felix Tejero¹, Lourdes Lorena Arias-Mota¹, Antonio Roschman-González², Pedro María Aso³ & Héctor José Finol²

ABSTRACT

Background: *Trypanosoma evansi* is the etiologic agent of the equine trypanosomiasis, a disease related to the detriment of the extensive bovine farming in the Venezuelan grasslands. Even though macroscopic pathologies such as anemia, pale mucosa, icteric tissues, generalized edema, splenomegaly, liver and renal hypertrophy, abortion, anoestrus, emaciation, lymphadenopathies, striated muscle atrophy as well as epicardiac and endocardiac hemorrhages have been described for infections with the agent, no reports of any heart ultrastructural change in experimental or natural infections induced by Venezuelan *T. evansi* isolates are available. So, a transmission electron microscopic approach to the problem was needed. This work describes cell features of the cardiac myocyte and the cardiac microvasculature ultrastructure in mice experimentally infected with an equine local isolate of *T. evansi*, also providing an account of the infection with the mice's survival.

Materials, Methods & Results: NMRI *Mus musculus* were inoculated with a Venezuelan *T. evansi* isolate derived from a naturally infected *Equus caballus*. From day three post-infection, and every other day until the mice's death, one rodent was randomly killed, the heart apex was isosmotically removed and cut in symmetrical blocks, which were fixed, post-fixed, dehydrated, infiltrated, included, sectioned, contrasted and studied by means of transmission electron microscopy, with the subsequent characterization of the cardiac myocyte and the cardiac microvasculature transformations. The evaluation of the micrographs demonstrated ultrastructural time-increasing harmful mitochondrial alterations that included reduction in the number of mitochondria per cell, decrease in mitochondrial dimensions and lessening of the number of cristae per mitochondrion. Myofibrillar destruction, myofilament loss and atrophy were also evident. In addition, damaging augmentation of the vascular endothelium thickness, appearance of abnormal endothelial projections and caveolae loss were incontestable changes. The presence of trypanosomes in the lumen of the heart capillary system was indubitable; however, neither intra-endothelial nor intra-cardiac myocyte parasites were observed; no inter-tissular parasites were found either.

Discussion: The ultrastructural modifications in the muscular heart tissue and in the heart capillaries of experimentally infected mice with a Venezuelan isolate of *T. evansi*, derived from a feral domesticated *E. caballus*, were incontrovertible being characterized by the deleterious gradual mitochondrial decline. In such a context, the close relationship between the mitochondrion and the ribosome disposition is related to protein synthesis being associated to diverse functions and stress reactions to non-proper substances like *T. evansi*, such circumstance could lead to cardiac myocyte mitochondrial deterioration. Additionally, changes in the mitochondrial dimensions and/or the number of cristae/mitochondrion are related to the mitochondrial enzyme activity. The myofilament loss and the myofibrillar destruction reported in this work could derive from the capillary damage per se. The overexpression of serum deprivation protein response induces caveolae deformation and endothelial cell membrane tubulation. The heart's myodamage could be additionally caused by autoimmunity and/or electrolytic unbalance induced by the trypanosome. The endothelial cell detriment could be the result of a distant effect of parasitic toxic catabolites, intense edema, hypoxia and/or ischemia. The atrophy was put in evidence by a growing volume reduction as a result of myofibril loss probably due to collateral ischemic and hypoxic mechanisms caused by the parasite. Furthermore, the effect due to toxins could cause intramuscular microvasculature damage, hypoxia and fibrillar atrophy. The trypanosomes were present in the cardiac capillary circulation, being able, as an inducible result of the liberation of active materials, to provoke mononuclear and polymorphonuclear infiltration, contributing to the inflammatory response. The subcellular damage in the cardiac myocytes and in the cardiac microvasculature, along with the presence of trypanosomes in the coronary circulation, and the lack of association between parasites and cardiac myocytes or parasites and cardiac endothelial cells, are attributes with a remarkable pathological meaning since it represents a non described phenomenon of gradual ultrastructural change that take part of the events, resulting in the murine host death through a degenerative mechanism.

Keywords: *Trypanosoma evansi*, cardiac muscle, cardiac microvasculature, murine infections, ultrastructure, pathology.

Received: February 2010

www.ufrgs.br/actavet

Accepted: May 2010

*This research was funded by FONACIT (Project G98-03462). ¹Instituto de Zoología y Ecología Tropical (IZET), Facultad de Ciencias, Universidad Central de Venezuela (UCV), Av. Paseo Los Ilustres. Los Chaguaramos. Caracas, Venezuela. ²Centro de Microscopía Electrónica, Facultad de Ciencias-UCV. ³Departamento de Biología Celular, Universidad Simón Bolívar (USB), Caracas, Venezuela. CORRESPONDENCE: F. Tejero [felix.tejero@ciens.ucv.ve; felixtejero@gmail.com - Phone/Fax: + 58 (0212) 605-1647].

INTRODUCTION

Trypanosoma evansi is the etiologic agent of the equine trypanosomiasis in the Venezuelan savannas, an area with more than 230,000 Km², mostly used for extensive bovine production. Horses are required to drive bovine herds; consequently, total or partial Creole feral domesticated horse disability implies losses in livestock production along with a negative socioeconomic impact to the region [32].

T. evansi is an eurixenous parasite with a diverse range of symptoms in the susceptible mammalian hosts, including anemia, pale mucosal and icteric tissues, generalized edema, splenomegaly, liver and renal hypertrophy [4], abortion [19], and anoestrus [27]. Additional harms also includes emaciation, lymphadenopathies, striated muscle atrophy, and epicardiac and endocardiac hemorrhages [1,2,7,12,40].

Even though the ultrastructural alterations induced by Venezuelan *T. evansi* isolates have been studied in the striated muscle of naturally infected wild horses [30], as well as in the skeletal muscle [9], liver [34,38], kidney [39] and adrenal gland [33] of mice under experimental conditions, nothing is known about its effects on the heart's musculature.

This work aimed to describe findings in the cardiac myocyte and cardiac microvasculature ultrastructural alterations in mice experimentally infected with an equine local isolate of *T. evansi*, relating it to the experimental host death.

MATERIALS AND METHODS

A *Trypanosoma evansi* isolate derived from a naturally infected *Equus caballus* [28] preserved in liquid nitrogen¹ [35] was inoculated in 30 sepsis, protozoan-, fungus-, helminthes- and ectoparasites-free outbred NMRI *Mus musculus* (Venezuelan Institute of Scientific Investigations breeding), divided in 3 groups of 10 mice each; one additional 10-mice group was used as a control. Mice (♀ 20 gr body weight) were maintained in plastic boxes (39 cm L × 20 cm W × 24 cm H; 10 mice/box) provided with rice husk bedding (every other day change), reverse osmosis treated tap water², and commercial dried concentrate food³ (two repositions/day), being husbanded in an environment with continuous clean air flow supply, controlled temperature (24-27°C), and humidity (75-85%) with 12 h of LED day-light illumination. Mice were intradermally injected

with 1 blood-free DEAE-cellulose⁴ column purified trypomastigote [16] per gram of mouse body weight suspended in 0.15 mL of the column's elution buffer⁵ (2.7 mM potassium chloride, 1.8 mM potassium phosphate, 137.0 mM sodium chloride, 10.1 mM sodium phosphate, 55.6 mM glucose). Prior to the inoculation, the purified trypanosomes were serially diluted in the elution buffer until the desired concentration (20 trypanosomes/0.15 mL); identical control animals were inoculated in the same conditions with *T. evansi*-free elution buffer.

From day 3 post-infection, and every other day during 15 days (at day 17 all mice died because of the *T. evansi* infection), one mouse from each group was randomly selected and killed in a saturated pure carbon monoxide⁶ chamber. By means of surgical ablation, the heart was removed and placed on a Petri dish containing Karnovsky [24] fixative solution at 4°C, pH 7.4 and 320 mOsm. The heart's apex was excised and systematically sectioned in 2 mm³ blocks which were fixed during 5 min in Karnovsky fixative, washed in Millonig buffer [23] for 5 min and post-fixed in 1% osmium tetroxide [24] for 60 min at the same temperature, pH and osmolarity. Subsequently, sample tissues were submerged in distilled water (15 min) and later dehydrated in an ethanol series of increasing concentrations: 50-70-90-95-100% (5 min each one at 4°C). After, the fragments were infiltrated with propylene oxide (2 changes 15 min/each), propylene oxide-epon⁷ (30 min), pure epon (4 changes of 30 min/each)[20] and included in epoxy resin (EMBed-812, DDSA, NMA, DMP-30) for 48 h/60°C. Diamond knife⁸ cut ultrathin sections⁹ (60-80 nm) were put on collodion covered¹⁰ 300 mesh copper grids¹¹ and contrasted with uranyl acetate [42] and lead citrate [31]. A transmission electron microscope¹² (80 kV) was used for observation and digital image recording.

All the experiments followed the guidelines established in the guide for the care and use of laboratory animals [15]. Experiments were repeated three times with different mice and parasite batches.

RESULTS

No sign of ultrastructural change was observed in the heart of the control mice (Figure 1A). Noticeable, in addition, was the fact that mitochondria had similar electron density.

From day 3 post-infection, successive and cumulative detrimental ultrastructural changes started

to emerge. The most remarkable signs were observed in the cardiac myocyte mitochondria, the myofibrillar structure, including myofilament loss, and the cardiac's capillary endothelium.

The mitochondrial change involved a reduction in the number of mitochondria per cell and a decrease in the mitochondria dimensionality (Figure 1. B-D; Figure 2. C-D). The number of cristae per mitochondrion also fell. Mitochondria presence in the subsarcolemmal and intermyofibrillar spaces was evident (Figure 2D). Intermyo-fibrillar autophagic vacuoles were likewise evident. The disorganization of myofibrils caused atrophy with an increment of subsarcolemmal and intermyofibrillar spaces (Figure 1. B-D; Figure 2. C-D). In some of those areas, swollen sarcotubular elements were present (Figure 1. B-C), while in others, such signs were absent (Figure 1. D).

The basement membrane was seen widened and electrondense in some sections (Figure 2. D).

Intramuscular capillaries showed endothelial cell cytoplasm with some widened areas, prolongations into the lumen, loss of caveolae, and pinocytic vesicles (Figure 1. C-D; Figure 2. A) exhibiting different degrees of lumen obliteration (Figure 2. B - D) and macrophages in the extracellular spaces (Figure 2. B). The presence of the parasite was obvious in the lumen of the intramuscular capillary system (Figure 2. C).

DISCUSSION

The results clearly demonstrated ultrastructural modifications in the muscular heart tissue, including the heart capillaries, of mice experimentally infected with a Venezuelan isolate of *Trypanosoma evansi* derived from a feral domesticated *Equus caballus*. On

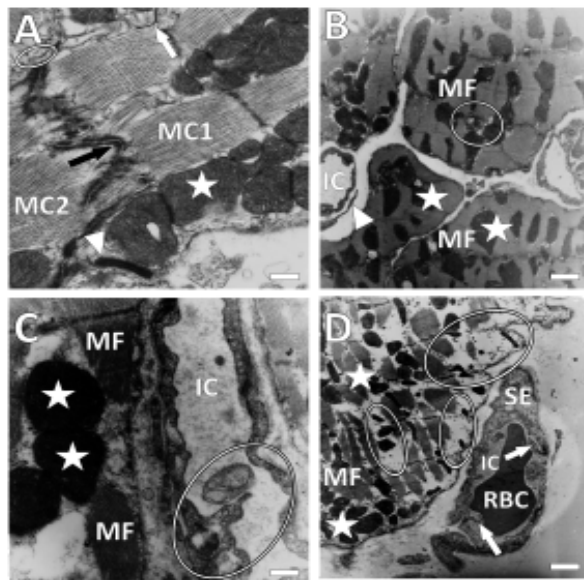


Figure 1. Ultrastructural change throughout the first week of infection. A. Control. Black arrow: fascia adherens; arrowhead: macula adherens; oval: caveolae with some elements of the sarcoplasmic reticulum; white arrow: gap junction; star: mitochondria (scale bar: 0.3 μ m). B. Day third post-infection. Oval: swollen mitochondrion; IC: intramuscular capillary; arrowhead: part of a Rouge cell; stars: mitochondria with different electron densities; MF: myofibrils (scale bar: 0.2 μ m). C. Day fifth post-infection. Stars: mitochondria; IC: intramuscular capillary; oval: long luminal endothelial projection with swollen endothelial cell showing caveolae and degenerated mitochondrion (scale bar: 0.5 μ m). D. Day seventh post-infection. Stars: groups of mitochondria; IC: intramuscular capillary; RBC: red blood cell; MF: myofibrils; SE: swollen endothelial cell with absence of caveolae and pinocytic vesicles; arrows: luminal endothelial projections; ovals: intermyofibrillar spaces lacking sarcotubular elements (scale bar: 0.15 μ m).

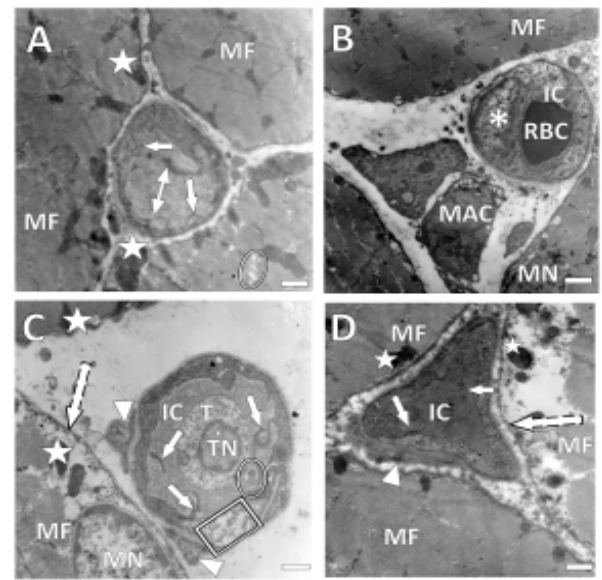


Figure 2. Change in the cardiac muscle during the infection's second week. A. Day ninth post-infection. MF: myofibrils; oval: swollen tubules of the sarcotubular system; arrows: luminal endothelial projections; stars: mitochondria (scale bar: 0.2 μ m). B. Day eleventh post-infection. MF: myofibrils; IC: intramuscular capillary; RBC: red blood cell; MAC: macrophage; asterisk: nucleus of the endothelial cell; MN: myonucleus (scale bar: 0.15 μ m). C. Day thirteenth post-infection. Star: mitochondria; discontinuous arrow: subsarcolemmal space; MF: myofibrils; MN: myonucleus; arrowheads: Rouge cells; IC: intramuscular capillary; arrows: luminal endothelial projections; rectangle: altered endothelial zone; T: trypanosome; TN: trypanosome nucleus; circle: trypanosome flagellum (scale bar: 0.25 μ m). D. Day fifteenth post infection. MF: myofibrils; stars: mitochondria; discontinuous arrow: widened subsarcolemmal space; arrowhead: Rouge cell; IC: intramuscular capillary; arrows: luminal endothelial projections (scale bar: 0.25 μ m).

the other hand, no changes were evident in mice inoculated with a parasite-free elution buffer (control).

The cumulative ultrastructural mitochondrial degeneration is an associated characteristic of change due to pathologies [6]. Keeping in mind that mitochondria location is related to specific ATP-requiring sites [41], and the products of mitochondrial protein biosynthesis are hydrophobic proteins located in the inner membrane, it is possible that the synthesis of these proteins could occur on associated ribosomes [18]. So, the close mitochondrion-ribosome disposition is related to an increase in the protein synthesis associated to an ample range of functions and stress reactions to non-proper substances, as snake venom [11], and as observed in our results, caused by *T. evansi*. Such stressful conditions could cause cardiac myocyte mitochondrial deterioration. Moreover, the presence of polymorphic and variable mitochondrial electron densities herein reported had already been described in harmful conditions such as rats under a food-restricted diet [26]. The variations in mitochondrial size and number of cristae per mitochondrion are features associated with changes in the mitochondrial enzyme activity [37].

The characteristically muscular myofibrillar disposition is an archetypal example of a form-function relationship. In this work, the atrophy with progressive volume reduction was put in evidence as a result of myofibril loss. Similar results were reported in *in vitro*-cultured mouse ventricular myocardial cells, where a low ethanol dose decreased the volumetric proportion of myofibrils [21]. Moreover, atrophy and myofibrillar destruction in the heart of *Crotalus* envenomed mice has also been described [11]. On the other hand, the myofilament loss and the myofibrillar destruction observed in our results could be explained by the capillary damage in the heart's vasculature. In such a context, the overexpression of serum deprivation protein response, unlike polymerase I, and transcript release factor may have induced caveolae deformation and extensive tubulation of the endothelial cell membrane, as previously reported [10].

The micrographs showed intermyofibrillar and subsarcolemal widened spaces, a clear indicator of atrophy. In addition, swollen tubules in the cardiac muscle sarcotubular system was also present. The phenomenon was described in rheumatoid arthritis [22] and in the skeletal musculature of natural [30] and experimental [9] local *Trypanosoma evansi* infections. Moreover, the lack of specificity of the

contractile and sarcotubular system modifications have been described in *Serinus canarius* under experimental *Plasmodium cathemerium* stress [5] being also characterized in diverse inflammatory myopathologies [8]. In addition, similar degenerative observations have been reported in the skeletal muscle of mice experimentally poisoned with *Crotalus vegrandis* venom [29].

Results showed atrophy probably due to indirect ischemic and hypoxic mechanisms induced by the parasite. Such hypothesis could also imply that the action of parasitic toxins may cause intramuscular microvasculature damage, hypoxia and fibrillar atrophy, unlike results that have been reported about horses experimentally infected with *T. evansi* [13]. Then, in the absence of muscular invasion, in addition to the lack of reports describing the cardiac myocyte as a *target* tissue in the life cycle of this trypanosomatid, the heart's myodamage could be additionally caused, as described in other pathologies, by autoimmunity [36] and/or electrolytic unbalance [3], probably induced by the trypanosome itself.

Endothelial cell damage was also evident in our results. The observed heart modifications could be indirectly due to the parasite since no trypomastigote was observed inside any kind of cardiac or endothelial cell. In the same context of distance damage, the collateral effects of local *T. evansi* has been demonstrated in the skeletal muscle of naturally infected wild horses [30] and experimentally infected laboratory mice [9]; no reports of any trypanosome located inside the skeletal muscular cells are available, but collectively, results from others gave an account of the parasites in the muscular vasculature. These results were consistent with ours.

The collateral vascular harm and hematic element damage seen in mice experimentally infected with *Trypanosoma evansi* were previously attributed to the action of proteolytic enzymes secreted by the parasite [33]. However, in such an indirect detrimental setting, the inflicted heart vasculature change could be caused by unknown parasitic toxic catabolites, causing, in turn, intense edema, hypoxic phenomena and/or ischemic processes driving the cells to death.

As the experimental infection advanced, the trypanosomes appeared in the cardiac capillary circulation, associated with inflammation by macrophages. Immune complexes could allow the release of active substances causing mononuclear and polymorphonuclear infiltration [14], being indicated

that such immune complexes are able to cause tissular damage and, therefore, contribute to inflammation [25]. Similar observations have been reported in equine acute rhabdomyolysis [17].

The described cascade of ultrastructural changes seen in this study suggests a distance injurious process with outstanding pathological significance, since it could play an undefined role requiring further investigation that is part of the episodes concluding with the murine host death through a progressive degenerative mechanism.

CONCLUSION

Results from this study put in evidence ultrastructural differences between controlled and experimentally *Trypanosoma evansi* infected mice. The heart's ultrastructural characteristics of the *T. evansi* infected mice was patent by means of an associated degenerative mechanism, including damage in the mitochondria of the cardiac myocyte, myofibrillar destruction, myofilament loss, atrophy, as well as detrimental increasing of the vascular endothelium thickness, abnormal endothelial projections and caveolae loss. Even though the trypanosomes were evident in the lumen of the heart capillary system, neither intra-endothelial nor intra-cardiac myocyte

parasites were observed. Such duality suggests a distance damage process involved in the phenomena, concluding with the death of the experimental hosts.

Acknowledgements. The financial support of the Fondo Nacional de Ciencia, Tecnología e Investigación is gratefully acknowledged.

SOURCES AND MANUFACTURERS

¹Liquid nitrogen. School of Physics, Faculty of Sciences, UCV, Caracas, Venezuela.

²Reverse osmosis RO-300. Pure Aqua, Inc. Santa Ana, USA.

³Ratarina. Protinal, Caracas, Venezuela.

⁴DEAE cellulose. Sigma-Aldrich, St. Louis, USA.

⁵All chemicals. Sigma-Aldrich, St. Louis, USA.

⁶Carbon monoxide. Oxia C.A., Caracas, Venezuela.

⁷Epon and all epoxy resins. Ladd Research, Williston, USA.

⁸Ultra 45° Diamond Knife. Diatome Diamonds Knives, Hatfield, USA.

⁹Ultramicrotome. MT-2 Sorval Porter Blum, Norwalk, USA.

¹⁰Collodion. Eastman Kodak Co., Rochester, USA.

¹¹Copper grids. Electron Microscopy Sciences, Hatfield, USA.

¹²Transmission electron microscope. JEM-1011, JEOL Ltd., Tokyo, Japan.

REFERENCES

- 1 Audu P.A., Esievo K.A., Mohammed G. & Ajanusi O.J. 1999.** Studies of infectivity and pathogenicity of an isolate of *Trypanosoma evansi* in Yankasa sheep. *Veterinary Parasitology*. 86(3): 185-190.
- 2 Biswas D., Choudhury A. & Misra K.K. 2001.** Histopathology of *Trypanosoma (Trypanozoon) evansi* infection in bandicoot rat. I. Visceral organs. *Experimental Parasitology*. 99(3): 148-159.
- 3 Briani C., Doria A., Saarzi-Puttini P. & Dalakas M.C. 2006.** Update on idiopathic inflammatory myopathies. *Autoimmunity*. 39 (3): 161-170.
- 4 Cadioli F.A., Marques L.C., Machado R.Z., Alessi A.C., Aquino L.P.C.T. & Barnabé P.A. 2006.** Experimental *Trypanosoma evansi* infection in donkeys: hematological, biochemical and histopathological changes. *Arquivo Brasileiro de Medicina Veterinária e Zootecnia*. 58(5): 749-756.
- 5 Carmona M., Finol H.J., Márquez A. & Noya O. 1996.** Skeletal muscle ultrastructural pathology in *Serinus canarius* infected with *Plasmodium cathemerium*. *Journal of Submicroscopic Cytology and Pathology*. 28(1): 87-91.
- 6 Calore E.E., Cavalieri M.J., Haraguchi M., Górniak S.L., Dagli M.L.Z., Raspantini P.C. & Calore N.M.P. 1997.** Experimental mitochondrial myopathy induced by chronic intoxication by *Senna occidentalis* seeds. *Journal of the Neurological Sciences*. 146(1): 1-6.
- 7 Damayarti R., Graydon R.J. & Ladds P.W. 1994.** The pathology of experimental *Trypanosoma evansi* infection in the Indonesian buffalo (*Bubalus bubalis*). *Journal of Comparative Pathology*. 110(3): 237-252.
- 8 de Palma L., Chillemi C., Albanelli S., Rapali, S. & Bertoni-Freddari C. 2000.** Muscle involvement in rheumatoid arthritis: an ultrastructural study. *Ultrastructural Pathology*. 24(3): 151-156.
- 9 Finol H.J., Boada-Sucre A., Rossi M. & Tejero F. 2001.** Skeletal muscle ultrastructural pathology in mice infected with *Trypanosoma evansi*. *Journal of Submicroscopic Cytology and Pathology*. 33(4): 65-71.

- 10 Hansen C.G., Bright N.A., Howard G. & Nichols B.J. 2009. SDPR induces membrane curvature and functions in the formation of caveolae. *Nature Cell Biology*. 11(7): 807-814.
- 11 Hernández M., Finol H.J., López J.C., Fernández I., Scannone, H. & Rodríguez-Acosta A. 2005. Alteraciones ultraestructurales de tejido cardíaco tratado con veneno crudo de serpiente de cascabel (*Crotalus durissus cumanensis*). *Revista de la Facultad de Medicina*. 28(1): 12-16.
- 12 Herrera H.M., Alessi A.C., Marques L.C., Santana A.E., Aquino L.P., Menezes R.F. Moraes M.A. & Machado R.Z. 2002. Experimental *Trypanosoma evansi* infection in South American coati (*Nasua nasua*): hematological, biochemical and histopathological changes. *Acta Tropica*. 81(3): 203-210.
- 13 Hörchner F., Schönefeld A. & Wüst B. 1983. Experimental infection of horses with *Trypanosoma evansi*. Parasitological and clinical results. *Annales de la Société belge de médecine tropicale*. 63(2): 127-135.
- 14 Igbokwe I.O. 1994. Mechanisms of cellular injury in African trypanosomiasis. *Veterinary Bulletin*. 64(7): 611-620.
- 15 Institute of Laboratory Animal Resources. 1996. Guide for the Care and Use of Laboratory Animals. Washington D.C.: National Academy Press, 140p.
- 16 Lanham S. & Godfrey D. 1970. Isolation of salivarian trypanosomes from man and other animals using DEAE cellulose. *Experimental Parasitology*. 28(3): 521-534.
- 17 Lindholm A., Jöhanesson H. & Kjaersgaard P. 1974. Acute rhabdomyolysis ("Tying-up") in Standardbred horses. A morphological and biochemical study. *Acta Veterinaria Scandinavica*. 15(3): 325-339.
- 18 Liu M. & Spremulli L. 2000. Interaction of mammalian mitochondrial ribosomes with the inner membrane. *Journal of Biological Chemistry*. 275(38): 29400-29406.
- 19 Lohr K.F., Pohlpark S., Siriwan P., Leesirikul N., Srikitjakoru L.P. & Staak C. 1986. *Trypanosoma evansi* infection in buffaloes in north-east Thailand. II. Abortions. *Tropical Animal Health and Production*. 18(2): 103-108.
- 20 Luft J.H. 1961. Improvements in epoxy resin embedding methods. *Journal of Biophysical and Biochemical Cytology*. 9(2): 409-414.
- 21 Mashimo K., Sato S. & Ohno M. 2003. Chronic effects of ethanol on cultured myocardial cells: ultrastructural and morphometric studies. *Virchows Archiv*. 442(4): 356-363.
- 22 Matsubara S. & Mair W.G.P. 1980. Ultrastructural changes of skeletal muscle in polyarteritis nodosa and arteritis associated with rheumatoid arthritis. *Acta Neuropathologica*. 50(3): 169-174.
- 23 Mausbach A.B. & Afzekius B.A. 1999. Fixative Vehicle. In: *Biomedical Electron Microscopy. Illustrated Methods and Interpretations*. London: Academic Press, pp.60-79.
- 24 Mausbach A.B. & Afzekius B.A. 1999. Fixatives. In: *Biomedical Electron Microscopy. Illustrated Methods and Interpretations*. London: Academic Press, pp.32-59.
- 25 Nielsen K.H. 1985. Complement in trypanosomiasis. In: *Immunology and Pathogenesis of Trypanosomiasis*. Boca Raton: CRC Press, pp.133-144.
- 26 Okoshi M.P., Okoshi K., Pai D.V., Pai-Silva M.D., Matsubara L.S. & Cicogna A.C. 2001. Mechanical, biochemical, and morphological change in the heart from chronic food-restricted rats. *Canadian Journal of Physiology and Pharmacology*. 79(9): 754-760.
- 27 Payne R.C., Sukanto I., Bazely K. & Jones T.W. 1993. The effect of *Trypanosoma evansi* infection on the oestrus cycle of Friesian Holstein heifers. *Veterinary Parasitology*. 51(1-2): 1-11.
- 28 Perrone T.M., Gonzatti M.I., Villamizar G., Escalante A. & Aso P.M. 2009. Molecular profiles of Venezuelan isolates of *Trypanosoma* sp. by random amplified polymorphic DNA method. *Veterinary Parasitology*. 161(3-4): 194-200.
- 29 Pulido-Méndez M., Rodríguez-Acosta A. Finol H.J., Aguilar I. & Girón M.E. 1999. Ultrastructural pathology in skeletal muscle of mice envenomed with *Crotalus vegrandis* venom. *Journal of Submicroscopic Cytology and Pathology*. 31(4): 555-561.
- 30 Quiñones-Mateu M.E., Finol H.J., Sucre L.E. & Torres S.H. 1994. Muscular changes in Venezuelan wild horses naturally infected with *Trypanosoma evansi*. *Journal of Comparative Pathology*. 110(1): 79-89.
- 31 Reynolds E.S. 1963. The use of lead citrate at high pH as an electron opaque stain in electron microscopy. *Journal of Cell Biology*. 17(1): 208-212.
- 32 Rivera M.A. 1996. *Hemoparasitosis bovinas*. 1a ed. Caracas: Universidad Central de Venezuela – Consejo de Desarrollo Científico y Humanístico, 237p.

- 33 Rossi M., Boada-Sucre A., Finol H.J., Tejero F., Aso P.M., Bello B. & Hernández G. 1999.** Ultrastructural alterations in the adrenal gland cortex of mice experimentally infected with a Venezuelan isolate of *Trypanosoma evansi*. *Journal of Submicroscopic Cytology and Pathology*. 31(4): 509-513.
- 34 Rossi M.S., Boada-Sucre A.A., Hernández G., Bello B., Finol H.J., Payares-Trujillo G. & Aso P.M. 2008.** Análisis ultraestructural del hígado en ratones infectados experimentalmente con un aislado venezolano de *Trypanosoma evansi* (Kinetoplastida: Trypanosomatidae). *Acta Microscopica*. 17(1): 5-12.
- 35 Schuster J.P., Mehlhorn H. & Raether W. 1996.** Ultrastructural changes on various *Trypanosoma* spp. after a 30-year storage period in liquid nitrogen. *Parasitology Research*. 82(8): 720-726.
- 36 Suber T.L., Casciola-Rosen L. & Rosen A. 2008.** Mechanisms of disease: autoantigens as clues to the pathogenesis of myositis. *Nature Clinical Practice Rheumatology*. 4(4): 201-209.
- 37 Tejero F. & Finol H.J. 2004.** *Trypanosoma rangeli*: ultrastructure and activity of the mitochondrion. *Journal of Submicroscopic Cytology and Pathology*. 36(3-4): 313-317.
- 38 Tejero F., Brun S., Roschman-Gonzalez A., Perrone-Carmona T.M., Aso P.M., Velasco E. & Finol H.J. 2009.** *Trypanosoma evansi*: analysis of the ultrastructural change in hepatic cells during murine experimental infections. *Acta Microscopica*. 18(1): 28-32.
- 39 Tejero F., Brun S., Roschman-Gonzalez A., Velasco E., Aso P.M. & Finol H.J. 2009.** Ultraestructura renal en infecciones marinas experimentales con un aislado venezolano de *Trypanosoma evansi*. *Revista del Instituto Nacional de Higiene "Rafael Rangel"*. 40(2): 44-49.
- 40 Uche U.E. & Jones T.W. 1992.** Pathology of experimental *Trypanosoma evansi* infection in rabbits. *Journal of Comparative Pathology*. 106(3): 299-309.
- 41 Wachter C., Schatz G. & Glick B.S. 1994.** Protein import into mitochondria: the requirement for external ATP is precursor-specific whereas intramitochondrial ATP is universally needed for translocation into the matrix. *Molecular Biology of the Cell*. 5 (4): 465-474
- 42 Watson M.L. 1958.** Staining of tissue sections for electron microscopy with heavy metals. *Journal of Biophysical and Biochemical Cytology*. 4(4): 475-478.